Eur Spine J (2007) 16:523–529
DOI 10.1007/s00586-006-0235-4

ORIGINAL ARTICLE

Pedicle growth asymmetry as a cause of adolescent idiopathic scoliosis: a biomechanical study

Anne-Marie Huynh · Carl-Eric Aubin · Talib Rajwani · Keith M. Bagnall · Isabelle Villemure

Received: 28 February 2006 / Revised: 13 August 2006 / Accepted: 13 September 2006 / Published online: 10 October 2006

Abstract Over the last century the neurocentral junction (NCJ) has been identified as a potential cause of adolescent idiopathic scoliosis (AIS). Disparate growth at this site has been thought to lead to pedicle asymmetry, which then causes vertebral rotation and ultimately, the development of scoliotic curves. The objectives of this study are (1) to incorporate pedicle growth and growth modulation into an existing finite element model of the thoracic and lumbar spine already integrating vertebral body growth and growth modulation; (2) to use the model to investigate whether pedicle asymmetry, either alone or combined with other deformations, could be involved in scoliosis pathomechanisms. The model was personalized to the geometry of a nonpathological subject and used as the reference spinal configuration. Asymmetry of pedicle geometry (i.e. initial length) and asymmetry of the pedicle growth rate alone or in combination with other AIS potential pathogenesis (anterior, lateral, or rotational displacement of apical vertebra) were simulated over a period of 24 months. The Cobb angle and local scoliotic descriptors (wedging angle, axial rotation) were assessed at each monthly growth cycle. Simulations with asymmetrical pedicle geometry did not produce significant scoliosis, vertebral rotation, or wedging. Simulations with asymmetry of pedicle growth rate did not cause scoliosis independently and did not amplify the scoliotic deformity caused by other deformations tested in the previous model. The results of this model do not support the hypothesis that asymmetrical NCJ growth is a cause of AIS. This concurs with recent animal experiments in which NCJ growth was unilaterally restricted and no scoliosis, vertebral wedging, or rotation was noted.

Keywords Idiopathic scoliosis · Biomechanical modeling · Growth modulation · Spine · Neurocentral junction

A.-M. Huynh · C.-E. Aubin (✉) · I. Villemure
Mechanical/Biomedical Engineering Department, Ecole Polytechnique, Montreal, Quebec, Canada
e-mail: carl-eric.aubin@polymtl.ca

A.-M. Huynh · C.-E. Aubin · I. Villemure
Sainte-Justine University Hospital Center, Research Center, Montreal, Quebec, Canada

T. Rajwani
Department of Radiology and Diagnostic Imaging, University of Alberta, Edmonton, Alberta, Canada

K. M. Bagnall
Department of Surgery, University of Alberta, Edmonton, Alberta, Canada

Introduction

Adolescent idiopathic scoliosis (AIS) is a complex three-dimensional (3D) deformation characterized by both lateral curvature of the spine and transverse rotation. Since 1909, authors have suggested asymmetrical growth at the neurocentral junction (NCJ) as a potential cause of AIS [8, 9, 12, 17, 32]. Asymmetric NCJ growth theory is established on three successive steps: (1) NCJ asymmetry is thought to produce pedicle asymmetry, (2) pedicle asymmetry is thought to produce vertebral rotation, and (3) vertebral rotation is thought to result in lateral curvature. Even after numerous clinical studies [8, 12, 15, 17, 27, 30, 32] and

animal experiments [2, 4, 13], this hypothesis still remains not conclusively validated.

The mechanism of vertebral rotation caused by a longer pedicle, as seen empirically in the porcine model [2], still needs to be clarified as well as the link between vertebral rotation resulting subsequently in lateral curvature. It has been suggested that vertebral rotation induced increase in pressure and inhibited growth on the concave side of the physeal vertebral growth plates [2]. This would result in the creation of wedged vertebrae and the development of scoliosis [2]. Once the initial deformity is present, scoliosis would evolve within a vicious biomechanical cycle involving asymmetrical loads caused by the onset of spinal deformity and vertebral growth modulation [25, 28].

Finite element (FE) models of the spine integrating growth and growth modulation have been used to understand the process of curve progression [3, 24, 28] and to evaluate different hypotheses for the pathogenesis of AIS [29]. Pathogenesis studied by Villemure et al. [29] consisted of shift or rotation at T8, which was assumed to be the apical vertebra of the future scoliosis. Those transformations at T8 included (1) 3 mm linear shift (laterally) in the frontal plane, (2) 3 mm linear shift (anteriorly) in the sagittal plane, and (3) 2° rotation in the transverse plane. However no FE model has explored, to the authors' knowledge, NCJ as a potential cause of AIS. To study the NCJ hypothesis, pedicle asymmetry should be tested alone or in conjunction with other deformations as it is possible that pedicle asymmetry acts in combination with additional mechanisms to result in scoliosis.

The first objective of this study was to incorporate pedicle growth and growth modulation into an existing FE model of the thoracic and lumbar spine already integrating vertebral body growth and growth modulation [28]. The model was used, in the second objective, to investigate whether pedicle asymmetry, either alone or combined with other deformations tested by Villemure et al. [29], would produce scoliosis.

Materials and methods

The biomechanical model used in this study has been modified from a previous model of the progression of vertebral and spinal deformities [28, 29]. The original model is summarized here as well as the modifications added to it.

Personalized finite element model of the spine

A personalized FE model of the spine was obtained using a multiview radiograph technique [1, 5, 28] of a nonpathological female subject (Fig. 1). The latter was used as the reference spinal configuration. The vertebrae and intervertebral discs were represented using 3D elastic beam elements. Each vertebral body (26 elements) was modeled by ten beam elements oriented longitudinally which were connected by a rigid cross-bar system of 16 beam elements. Of the ten elements oriented longitudinally, eight were distributed along the vertebral edge in order to evaluate the distribution of internal stresses within the vertebral bodies as a mean to represent their wedge shape (Fig. 1c). The

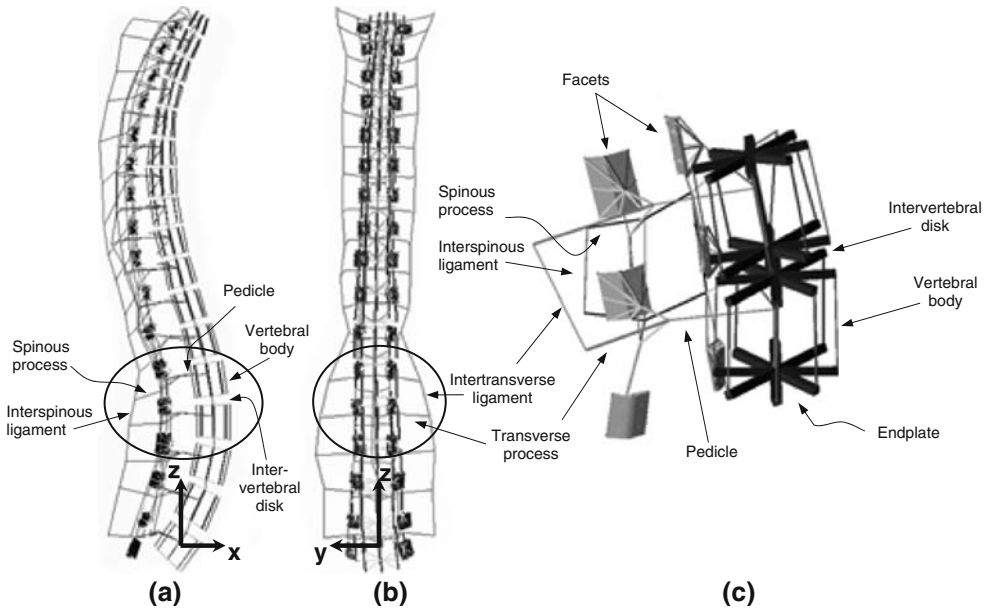

Fig. 1 Finite element model of the thoracic and lumbar spine in **a** lateral view, **b** postero-anterior view, and **c** details of a vertebral motion segment

pedicles of the vertebra were represented by single beam elements and were connected to one of the two center beams in the vertebral body. The pedicle beams were located in the middle of the two 3D coordinates of pedicle landmarks (superior and inferior pedicle extremity) from X-rays. The geometry (length) of these beams was adjustable in order to create right/left asymmetries. The posterior arches and the processes were also represented with the use of beam elements and the zygapophyseal joints were modeled with shell, spring, and point-to-surface contact elements. The ligaments were represented using springs. The mechanical properties were based on past experimental studies on cadaveric specimens [6]. The model was generated using ANSYS 7.0 finite element package (ANSYS Inc., USA).

The global axis system used was defined by three perpendicular axes corresponding to the anterior (X), left (Y), and upward (Z) directions. A consistent local axis for each vertebra was used where the x-axis was defined perpendicular to the superior and inferior growth plate and the y- and z-axis parallel to the growth plates.

Modeling of bone growth and growth modulation

Global growth was modeled as a combination of a baseline growth component and a growth modulation one. According to the research conducted by Stokes and Laible [24], longitudinal growth over a period of time is defined by growth strain increments, and deformation increments ($\delta\varepsilon$) due to growth modulation are described by $\delta\varepsilon = \beta\sigma(\delta G)$; where ($\delta G$) is the baseline growth, σ the internal stresses representing the biomechanical stimulus, and β the sensitivity of the bone tissue to that stimulus. The value of the sensitivity factor (β) was fixed to the one used by Villemure et al. [29] ($\beta = 0.6\ \mathrm{MPa}^{-1}$). The latter was obtained empirically from the FE model and was based on a physiological rationale restraining the amplitude of growth modulation produced within a cycle by the magnitude of the integrated growth increment [29]. Since the bone was represented by a beam element, the deformation $\delta\varepsilon$ can be simulated by applying equivalent internal forces δF_{M} based on the bone stiffness (represented by the Young modulus E): $\delta F_{\mathrm{M}} = \beta(EF_{\mathrm{M}})\delta G$. Internal forces ($F_{\mathrm{M}}$) are calculated from simulations of the model in response to a specific loading condition. Longitudinal growth and growth modulation were applied to the vertebral bodies and the pedicles.

Growth and growth modulation were considered separately in a stepwise iterative procedure where one iteration represented 1 month. Growth included first the application of a monthly growth increment and followed by the update of the spine by relocation of the model nodes. The monthly growth increments of the vertebral body were adapted from published data of 0.8 and 1.1 mm/year for the thoracic and lumbar vertebrae, respectively [7, 26]. The monthly growth rate of the pedicles was derived from experimentally determined value of 0.1 mm/year [7]. Alternate pedicle growth rates (up to six times more) were tested, but their effects did not affect the conclusion of this study. Following these two steps integrated in the growth component, growth modulation forces were applied and the geometry was updated based on these forces. This cycle was repeated over 24 months.

In this study, it is assumed that growth modulation results from a modification or a shift from the normal loads evaluated on the reference spine with the latter remaining constant throughout the entire simulation. The gravity loads associated with each vertebral level were based on measurements taken by Schultz et al. [19] and amplified based on the research of Nachemson [11] in order to include the muscular component for an upright standing subject. The loads were applied to the center of the superior vertebral endplate along the global z-axis and remained constant during all cycles. Internal stresses σ and σ', respectively, generated in the reference configuration and altered scoliotic profile were used to compute the differential stress state $\Delta\sigma = \sigma' - \sigma$ and hence generate growth modulation [28, 29]. For each simulation, all degrees of freedom were fixed at L5 and lateral flexion, forward flexion, and vertical translation were permitted at T1. Sensitivity studies showed that alternated boundary conditions (more or less constraining) at T1 did not significantly alter the model results.

Simulations

Pedicle asymmetries were simulated alone and in combination with the three potential pathogeneses tested by Villemure et al. [29] and presented in Introduction. Of the original scenarios tested by Villemure et al. [29], only the rotation of T8 was increased to 5° instead of 2° as this was thought to more accurately represent the degree of vertebral rotation potentially seen at the apex of a scoliotic curve [18].

Two different types of pedicle asymmetry were modeled and tested on both the right and left pedicles. (1) Asymmetry of the pedicle growth rate (i.e. one pedicle growing at the normal rate and the other failing to grow) was simulated to investigate the effects that occurred during the development of the asymmetry. In addition, asymmetry of the pedicle geometry (one

pedicle with 0.5, 1.0, or 1.5 cm greater length) was modeled to assess any effects of pedicle asymmetry after the asymmetry had already manifested. One and a half centimeter in length between two pedicles was estimated to represent the maximal potential degree of pedicle asymmetry as this represents approximately ten times the asymmetry noted in morphometric analysis of AIS vertebrae [14]. (2) Asymmetry of pedicle geometry was simulated using three configurations: 1.5 cm longer pedicle at T8, graded asymmetry (T6 and T10 with 0.5 cm pedicle length asymmetry, T7 and T9 with 1.0 cm pedicle length asymmetry, and T8 with 1.5 cm pedicle asymmetry), and constant asymmetry (T6–T10 presenting constant 1.5 cm pedicle length asymmetry). The graded asymmetry scenario was simulated to investigate if the extent of pedicle length asymmetry corresponded to the location of the apical vertebra in any subsequent scoliosis created.

The Cobb angle and local scoliotic descriptors at T8 (maximum wedging angle, axial rotation) were assessed at each growth cycle. The latter were calculated by an in-house computer program to eliminate intraobserver and interobserver variation. This computer program used the location of the FE model nodes after each cycle (month) to calculate the indices (Cobb angle: angle between the perpendiculars at the inflexion points of the spinal curve in the frontal place, maximum wedging angle: angle between the two endplates in the plane of maximum deformity of the vertebra, axial rotation: analytical method adapted from Stokes et al. [23]). Based on standard conventions [10], a lateral curve with values greater than 10° of Cobb angle was characterized as a scoliosis. Vertebral rotation (θ_z) was defined with a positive value when in the counterclockwise rotation and a negative value when in the clockwise rotation viewed from above the vertebra [23, 29].

Results

Results obtained from the same extent and type of deformity on the right pedicle in one simulation and on the left pedicle in another simulation were not equal. This was expected as the reference spinal configuration came from a real nonpathological subject and slight variations in vertebral geometry symmetry are anticipated.

Asymmetry of pedicle simulated alone

Asymmetries of growth rate alone in the pedicles did not generate significant growth modulation forces in the vertebral bodies. Therefore, only asymmetries of pedicle geometry without the addition of other deformations were tested.

All three cases tested for geometric pedicle asymmetry (longest pedicle at T8, constant and graded differences in pedicle length from T6 to T10) did not change the initial Cobb angle (0.3°) by more than 0.9°. The rotation and wedging at the vertebral levels where pedicle geometry had been altered were not changed.

Asymmetry of pedicle combined with deformations tested by Villemure et al. [29]

The six simulations of pedicle geometry asymmetry and the six simulations of pedicle growth asymmetry added to the scenarios tested by Villemure et al. [29] (anterior, lateral, and rotational displacement of T8) did not significantly change the maximal wedging angle (maximum delta of 0.6°) and the vertebral rotation (maximum delta of 2.3°) beyond those created by the given displacement (Table 1). The Cobb angle only increased considerably for the simulation of the right

Table 1 Indices computed after 1 month, 12 months, and 24 months of original scenarios tested by Villemure et al. [29] and in conjunction with asymmetry of pedicles geometry and growth rate

Scenarios (applied at T8)	Month	Simulated scenarios of Villemure et al. [29]			Asymmetry of pedicle geometry						Asymmetry of pedicle growth					
					Longer left pedicle			Longer right pedicle			Left pedicle growth			Right pedicle growth		
		Cobb	θ_z	W	Cobb	θ_z	W	Cobb	θ_z	W	Cobb	θ_z	W	Cobb	θ_z	W
3 mm anterior shift	1	0.3	–0.9	1.6	–5.2	–0.9	1.6	4.2	–0.9	1.6	0.2	–0.9	1.6	0.3	–0.9	1.6
	12	–3.4	–0.8	1.8	–5.6	–0.7	1.8	3.6	–0.7	1.8	–7.5	–0.8	1.8	0.0	–0.8	1.8
	24	–10.3	–0.4	2.7	–10.3	0.0	2.8	1.3	0.1	2.7	–11.4	–0.2	3.0	–10.0	–0.3	2.7
3 mm shift to the right	1	2.6	–0.9	1.5	–2.8	–0.9	1.5	6.8	–0.9	1.5	2.6	–0.9	1.5	2.6	–0.9	1.5
	12	9.0	–1.7	0.3	5.9	–1.9	0.4	12.5	–2.0	0.4	9.1	–1.7	0.4	8.9	–1.7	0.4
	24	35.4	–5.4	7.7	40.3	–7.7	7.6	37.7	–7.5	7.6	37.6	–5.4	7.5	35.2	–5.7	7.3
5° rotation	1	–7.8	–5.9	1.6	–8.4	–5.9	1.6	1.6	–5.9	1.6	–7.8	–5.9	1.6	–7.8	–5.9	1.6
	12	–10.7	–5.7	2.6	–11.2	–5.1	2.5	–4.4	–5.1	2.5	–10.1	–5.6	2.6	–10.3	–5.6	2.6
	24	–33.2	–3.5	7.3	–28.8	–2.3	6.7	–33.7	–2.0	6.8	–28.5	–3.8	7.3	–31.2	–3.6	7.3

Cobb angle (Cobb), rotation (θ_z), and maximal vertebral wedging (W) are in degrees

pedicle asymmetry (maximum delta of 11.6°). For the three computed indices, the changes compared to Villemure et al. [29] results were generally greater for the asymmetry of pedicle geometry than the asymmetry of pedicle growth rate.

The Cobb angle, wedging, and rotation progressed in a nonlinear manner, with change in all three parameters being more important from 12 to 24 months than from 0 to 12 months. The monthly evolution of the scoliotic descriptors was not amplified significantly when pedicle asymmetry was included and compared to the results obtained by Villemure et al. [29] (Table 1, columns 3–5).

Discussion

To the authors knowledge, this is the first study to test the hypothesis that pedicle asymmetry might lead to the production of scoliosis using a spine FE model integrating growth and growth modulation of the vertebrae and the pedicles. The results obtained showed that pedicle asymmetry did not generate scoliotic deformity independently and did not amplify scoliosis caused by other deformations.

A pedicle length difference either modeled as a graded asymmetry or as a constant geometric asymmetry was not sufficient to generate critical forces. The latter created by the differences in length did not exert enough torque on the vertebral body to cause any degree of rotation. These findings conflict with the suggestion formulated by authors based on results from old anatomic studies of normal [20, 27] and scoliotic vertebrae [8, 12, 27, 30] that a longer pedicle typically causes vertebral body rotation. In these anatomic studies, despite the findings that pedicle asymmetry and rotation presented together in a characteristic manner, it could not be inferred whether pedicle asymmetry was the cause or the result of the vertebral rotation. This suggests that geometric asymmetry of the pedicle was not an independent cause of scoliosis.

The effects of geometric or growth asymmetry of the pedicle did not amplify the spinal and vertebral deformations created by the pathogenesis hypotheses tested by Villemure et al. [29]. On the basis of this study, pedicle asymmetry did not act in conjunction with other deformations to initiate scoliosis.

The asymmetry of pedicle growth rate alone was not sufficient to cause scoliosis independently. This concurs with recent animal experiments in which the NCJ growth was unilaterally restricted and no scoliosis vertebral wedging or rotation was noted [16]. In addressing the second step of the asymmetric NCJ growth theory (i.e. vertebral rotation caused by pedicle asymmetry), this study has shown that the pedicle asymmetry was not sufficient to produce vertebral rotation, even if the difference in length modeled exceeded ten times the normal amount of pedicle asymmetry noted in AIS patients [14]. Looking at the third step of the theory (lateral curvature created from vertebral rotation), a rotation of 5° of T8 produced lateral curvature. However, the cause of this vertebral rotation was not generated by pedicle asymmetry and therefore, these results cannot be inferred to support the specific theory of asymmetric NCJ growth. The lateral displacement of T8 also produced a scoliotic pattern typically seen in AIS (a primary thoracic curve combined with a secondary left lumbar curve). This supports, however, the hypothesis that the coronal balance of the spine is quite unstable [31] and not the asymmetric NCJ growth theory.

With the biomechanical model developed in this study, only the last two steps of the NCJ theory can be evaluated. However, experimental work involving the placement of pedicle screws unilaterally across the NCJ in the pig model [16] has demonstrated that the NCJ does not contribute as much as traditionally thought to the pedicle growth. Furthermore, it has been shown that the NCJ activity decreases over the course of development suggesting that the contribution of the NCJ to the pedicle growth may be minimal during adolescence. Before the asymmetric NCJ growth theory can be disproved, more research should be done on the porcine model developed by Beguiristain [2] in which it was found that unilateral placement of pedicle screws across the T6–T10 vertebrae resulted in the generation of scoliosis.

The method for measuring the axial rotation of vertebrae used is based on the offset from the vertebral body center and an estimate measured on X-rays in a scoliotic population [23]. As there were no modifications of the rotation following simulations of asymmetries of pedicle length alone, this method of calculating the axial rotation may not be adequate. However, the general conclusions on pedicle asymmetry concerning initiation factor for scoliosis should not be affected, as forces generated by pedicle asymmetry in the vertebral body were low. To further investigate the NCJ hypothesis, the addition of the growth in the NCJ would be beneficial. The growth at the NCJ site might exert a greater torque on the vertebral body than growth at the pedicle site. However to achieve this model, precise data on NCJ growth contribution during the adolescent period would be required.

Limits of the model also include the adjustment of the sensitivity parameter β in the FE model. Data are limited to the experiments on growth plates conducted by Stokes [21] on different anatomical sites and animal species. A range of growth sensitivity to stress was found, but specific data to vertebral human growth plate still need to be established. The simplified representation of the intervertebral disc (one beam) restricts its possible adaptation due to mechanical loads. It has been shown on the rat tails that disc thickness can be mechanically modulated during growth, which is similar to the growth modulation of human bone [22]. In this model, intervertebral disc growth was not included since prior studies have shown that the mean growth of the disc was less than 0.3 mm/year [28, 29]. The representation of the wedge shape of the intervertebral discs following a biomechanical stimulus can still be achieved by modeling the disc in a similar fashion to the vertebral bodies (i.e. center element with beams distributed along the edge) [3] in order to enable the evaluation of internal stresses variation within the disc.

Conclusion

From the results obtained, geometric or growth rate asymmetry of the pedicle was not an independent cause able to generate a scoliosis. Geometric or growth rate asymmetry of the pedicle did not increase the severity of scoliosis, rotation, or wedging created by anterior, lateral, or rotational eccentricity of T8. On the basis of this study, pedicle asymmetry did not act in conjunction with other deformations to initiate scoliosis. Therefore, this study does not support the hypothesis that asymmetrical NCJ growth is a cause of AIS.

Acknowledgments This work was supported by the Canadian Institutes of Health Research (CIHR), the CIHR Training Program in Mobility and Posture Disorders, the Alberta Provincial CIHR Training Program in Bone and Joint Health, the Réseau Provincial de Recherche en Adaptation-Réadaptation, and the Alberta Heritage Foundation for Medical Research. The scientific and technical assistance of Josée Carrier is gratefully acknowledged.

References

1. Aubin CE, Descrimes JL, Dansereau J, Skalli W, Lavaste F, Labelle H (1995) Geometrical modeling of the spine and the thorax for the biomechanical analysis of scoliotic deformities using the finite element method. Ann Chir 49:749–761
2. Beguiristain JL, De Salis J, Oriaifo A, Canadell J (1980) Experimental scoliosis by epiphysiodesis in pigs. Int Orthop 3:317–321
3. Carrier J, Aubin CE, Villemure I, Labelle H (2004) Biomechanical modelling of growth modulation following rib shortening or lengthening in adolescent idiopathic scoliosis. Med Biol Eng Comput 42:541–548
4. Coillard C, Rhalmi S, Rivard CH (1999) Experimental scoliosis in the minipig: study of vertebral deformations. Ann Chir 53:773–780
5. Delorme S, Petit Y, de Guise JA, Labelle H, Aubin CE, Dansereau J (2003) Assessment of the 3-D reconstruction and high-resolution geometrical modeling of the human skeletal trunk from 2-D radiographic images. IEEE Trans Biomed Eng 50:989–998
6. Descrimes JL, Aubin CE, Boudreault F, Skalli W, Zeller R, Dansereau J, Lavaste F (1995) Modelling of facet joints in a global finite element model of the spine: mechanical aspects. Three dimensional analysis of spinal deformities. IOS Press, pp 107–112
7. Diméglio A, Bonnel F (1990) Le rachis en croissance: scoliose, taille assise et puberté. Springer, Berlin Heidelberg New York
8. Knutsson F (1963) A contribution to the discussion of the biological cause of idiopathic scoliosis. Acta Orthop Scand 33:98–104
9. Michelsson JE (1963) The development of spinal deformity in experimental scoliosis. Acta Orthop Scand 33:91–97
10. Morrissy R, Weinstein SL (2001) Lovell and Winter's pediatric orthopaedics. Williams & Wilkins, Philadelphia
11. Nachemson A (1964) The load on lumbar disks in different positions of the body. Clin Orthop 45:107–122
12. Nicoladoni C (1909) Anatomie und mechanismus der skoliose. Urban and Scwarzenburg, Munchen
13. Ottander HG (1963) Experimental progressive scoliosis in a pig. Acta Orthop Scand 33:91–97
14. Parent S, Labelle H, Skalli W, de Guise J (2004) Vertebral wedging characteristic changes in scoliotic spines. Spine 29:E455–E462
15. Rajwani T, Bhargava R, Moreau M, Mahood J, Raso VJ, Jiang H, Bagnall KM (2002) MRI characteristics of the neurocentral synchondrosis. Pediatr Radiol 32:811–816
16. Rajwani T, Huang EM, Clark M, Secretan C, Woo A, Bhargava R, Moreau M, Lambert R, Videman T, Bagnall KM (2004) Using a porcine model to explore asymmetric pedicle growth as a cause of scoliosis. Research into spinal deformities 5. IOS Press, pp 95–98
17. Roaf R (1966) The basic anatomy of scoliosis. J Bone Joint Surg Br 48:786–792
18. Russell GG, Raso VJ, Hill D, McIvor J (1990) A comparison of four computerized methods for measuring vertebral rotation. Spine 15:24–27
19. Schultz A, Andersson GB, Ortengren R, Bjork R, Nordin M (1982) Analysis and quantitative myoelectric measurements of loads on the lumbar spine when holding weights in standing postures. Spine 7:390–397
20. Sevastik B, Xiong B, Sevastik J, Hedlund R, Suliman I (1995) Vertebral rotation and pedicle length asymmetry in the normal adult spine. Eur Spine J 4:95–97
21. Stokes IA (2002) Mechanical effects on skeletal growth. J Musculoskelet Neuronal Interact 2:277–280
22. Stokes IA, Aronsson DD, Spence H, Iatridis JC (1998) Mechanical modulation of intervertebral disc thickness in growing rat tails. J Spinal Disord 11:261–265
23. Stokes IA, Bigalow LC, Moreland MS (1986) Measurement of axial rotation of vertebrae in scoliosis. Spine 11:213–218

24. Stokes IA, Laible JP (1990) Three-dimensional osseo-ligamentous model of the thorax representing initiation of scoliosis by asymmetric growth. J Biomech 23:589–595
25. Stokes IA, Spence H, Aronsson DD, Kilmer N. (1996) Mechanical modulation of vertebral body growth. Implications for scoliosis progression. Spine 21:1162–1167
26. Taylor JR (1975) Growth of human intervertebral discs and vertebral bodies. J Anat 120:49–68
27. Taylor JR (1983) Scoliosis and growth. Patterns of asymmetry in normal vertebral growth. Acta Orthop Scand 54:596–602
28. Villemure I, Aubin CE, Dansereau J, Labelle H (2002) Simulation of progressive deformities in adolescent idiopathic scoliosis using a biomechanical model integrating vertebral growth modulation. J Biomech Eng 124:784–790
29. Villemure I, Aubin CE, Dansereau J, Labelle H (2004) Biomechanical simulations of the spine deformation process in adolescent idiopathic scoliosis from different pathogenesis hypotheses. Eur Spine J 13:83–90
30. Vital JM, Beguiristain JL, Algara C, Villas C, Lavignolle B, Grenier N, Senegas J (1989) The neurocentral vertebral cartilage: anatomy, physiology and physiopathology. Surg Radiol Anat 11:323–328
31. White AA III (1971) Kinematics of the normal spine as related to scoliosis. J Biomech 4:405–411
32. Yamazaki A, Mason DE, Caro PA (1998) Age of closure of the neurocentral cartilage in the thoracic spine. J Pedatr Orthop 18:168–172